Polystyrenes with Hydrophilic End Groups: Synthesis, Characterization, and Effects on the Self-Assembly of Breath Figure Arrays

ARTICLE *in* THE JOURNAL OF PHYSICAL CHEMISTRY B · JANUARY 2014

Impact Factor: 3.3 · DOI: 10.1021/jp4114392 · Source: PubMed

4 AUTHORS, INCLUDING:

Liangwei Zhu
Zhejiang University
11 PUBLICATIONS **126** CITATIONS
SEE PROFILE

Zhi-Kang Xu
Zhejiang University
251 PUBLICATIONS **6,271** CITATIONS
SEE PROFILE

THE JOURNAL OF PHYSICAL CHEMISTRY B

Article

pubs.acs.org/JPCB

Polystyrenes with Hydrophilic End Groups: Synthesis, Characterization, and Effects on the Self-Assembly of Breath Figure Arrays

Liang-Wei Zhu, Yang Ou, Ling-Shu Wan,* and Zhi-Kang Xu

MOE Key Laboratory of Macromolecular Synthesis and Functionalization, Department of Polymer Science and Engineering, Zhejiang University, Hangzhou 310027, China

Supporting Information

ABSTRACT: We report the synthesis and characterization of a series of hydroxyl-end-functionalized polystyrenes (PS−OH) and the formation of patterned porous films. The polymers were synthesized by chain end reaction of polystyrene having a bromide end group (PS−Br) with hydramines including ethanolamine, diethanol amine, 2-amino-1,3-propanediol, and 2-(2-aminoethoxy) ethanol. The polymers were characterized by gel permeation chromatography (GPC), nuclear magnetic resonance (NMR), matrix-assisted laser desorption ionization time-of-flight mass spectrometry (MALDI-TOF MS), and differential scanning calorimetry (DSC). It was found that the end groups can influence the glass transition temperature (T_g) of the polystyrenes. The polymers with different end groups were then used to prepare honeycomb-patterned porous films by the breath figure method. Results reveal that the subtle chain-end modification leads to a dramatic change in the morphology of the films. Honeycomb films with large area ordered structure can be easily prepared from PS−OH. Effects of the end groups as well as blending PS−OH with PS−Br on the surface pore diameter, pore center distance, and the hierarchical structure were studied in detail. As supported by the results of polymer hydrophilicity, *in situ* observation of the film formation process, as well as the chain mobility, the film structure is supposed to be mainly determined by the precipitation of polystyrene at the solution/water droplet interface and the interfacial activity enhanced by the end groups.

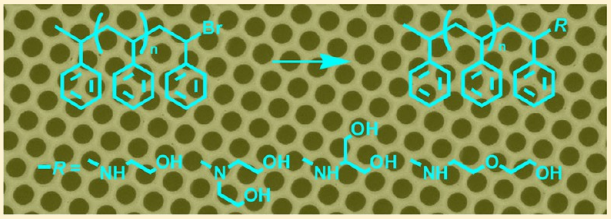

INTRODUCTION

The breath figure process has been widely used to prepare highly ordered porous films using self-organized water droplets as templates.[1] In this process, polymer solution with volatile solvent is cast on a substrate under humid conditions. As the solvent evaporates, water droplets condense onto the solution surface, grow bigger, form a stable polymer/water interface, and arrange into hexagonally close-packed three-dimensional arrays. After the solvent and water thoroughly evaporate, a honeycomb film is finally formed. Thanks to the cost efficiency and simple operation of the breath figure method, the resultant ordered films have shown a wide range of potential applications in fields of catalysis,[2,3] microcontainers,[4,5] photoelectronics,[6−8] sensors,[9] superhydrophobic surfaces,[10−12] biomaterials,[13−15] and separation membranes.[16−18]

The properties and functions of honeycomb films depend on the physical morphologies as well as the chemistry. For example, highly ordered micrometer-sized porous films can be used as surfaces guiding cell growth[19] or templates for fabricating microlens arrays,[20] while nanometer-sized films are desirable for photonic applications.[21] Through-pore films with highly uniform pores are able to precisely separate particles with different diameters.[16] Moreover, surface wettability of honeycomb films can be controlled by both surface chemistry and surface topology.[22−24] It has been reported that the structure of honeycomb films, such as pore size, pore shape, and monolayer/multilayer stacking, is affected by a series of factors, which include air flow rate, relative humidity, solvent property, solution concentration, substrates, and polymer structure.[25−27] For example, we found that the pores changed from near-spherical to ellipsoidal shape by introducing water-soluble polymers as additives or using water mixable solvent.[28] Shimomura, Hao, and our group demonstrated that using water or ice as substrates resulted in through-pore honeycomb films.[16,29,30] A typical example demonstrating the effects of polymer structure and solvent is that polystyrene without any polar groups can form ordered porous film only when the solvent is chloroform; however, polystyrene with polar end groups or polar blocks works well in carbon disulfide that is commonly used.[25,31,32]

Specifically, polymer structures can affect the morphologies of the films. A variety of polymers, including linear polymers,[6,33] star polymers,[7,11] comb polymers,[22,33] and dendritic polymers,[34] have been used to fabricate honeycomb films with different structures and properties. Stenzel et al. reported that the pore size dramatically decreased from 1 μm to 250 nm when the number of the arms of the star polymers increased from 5 to 18 by maintaining an equivalent star

Received: November 20, 2013
Revised: January 5, 2014
Published: January 8, 2014

   dx.doi.org/10.1021/jp4114392 | J. Phys. Chem. B 2014, 118, 845−854

molecular weight.[35] They also found that a five-arm star polymer with a hydrophobic end group of pentadecafluoro-1-octanolate led to films with smaller pore diameter (450 nm) than that with a bromide end group (750 nm).[35] Qiao et al. synthesized and compared star polymers with hydrophilic or hydrophobic (e.g., hydroxyl and pentadecafluorooctanoyl) end groups. They proposed that the difference in the polymer structures significantly changed the pore shape,[36] the effect of which is very similar to our results using water-soluble additives or solvents.[28]

In our previous work, we also found that honeycomb films prepared from a four-arm star polystyrene have a significantly different structure when compared with those from stars with a very short hydrophilic block.[37] Such polymers possess obviously different structures, i.e., with or without polar groups. In addition, as we know, it is difficult to know the polymerization degree of the second block in each arm due to the broad polydispersity and possible star−star coupling. In other words, the star polymer does not have a definite structure. In this work, we aimed to fine-tune polymer structure by synthesizing polystyrene with a series of hydrophilic end groups that have highly similar structure, and demonstrate the effects of these end groups on the formation and morphologies of the honeycomb films. Results indicate that even very similar hydrophilic end groups can induce great changes in film morphologies. This work may be helpful for putting an additional and unique brick in the understanding of the breath figure method and providing a method to control the hierarchical structure of honeycomb films.

EXPERIMENTAL SECTION

Materials. *N*,*N*,*N*′,*N*′,*N*′-Pentamethyldiethylenetriamine (PMDETA, Aldrich) was distilled from calcium hydride and stored at room temperature in a desiccator. Styrene (St) was obtained from Sinopharm Chemical Reagent Co. and distilled under reduced pressure before use. 1-Bromoethyl benzene (PEBr, 97%, Aldrich) was used without further purification. Copper(I) bromide (CuBr) was stirred in glacial acetic acid overnight, filtered, and washed with absolute ethanol under an argon blanket. The compound was dried under reduced pressure at 60 °C overnight. Ethanolamine, diethanolamine, 2-amino-1,3-propanediol, and 2-(2-aminoethoxy)ethanol (Sinopharm Chemical Reagent Co., analytical grade) were used as received. Deuterated chloroform ($CDCl_3$, 99.9%) was purchased from Sigma. Poly(ethylene terephthalate) (PET) film was kindly provided by Hangzhou Tape Factory and cleaned with acetone for 2 h before use. Water used in all experiments was deionized. All other chemicals were analytical grade and used as received.

Synthesis of PS−Br. The procedure used for synthesizing linear polystyrene with bromide end group, PS−Br, is as follows. ATRP of styrene was performed with a ratio of St/PEBr/CuBr/PMDETA = 200/1/1/2. A 50 mL Schlenk flask was charged with PEBr (0.87 mmol, 118.7 μL), PMDETA (1.74 mmol, 363 μL), and St (173.91 mmol, 20 mL) under a nitrogen atmosphere. The solution was degassed by three freeze−pump−thaw cycles. Then, CuBr (0.87 mmol, 125 mg) was added and another two freeze−pump−thaw cycles were performed. The polymerization was allowed to proceed at a preheated 100 °C oil bath. After 40 min, the flask was quenched in liquid nitrogen to stop the polymerization. The reaction mixture was dissolved with a small amount of tetrahydrofuran (THF), precipitated in methanol, and repeated three times. The obtained product was dried in a vacuum overnight. The monomer conversion was kept at as low as 27% to avoid losing the bromide end group. ^{1}H NMR (500 MHz, $CDCl_3$) δ (ppm): 7.26−6.2 (5H, C_6H_5), 4.6−4.4 (2H, CH_2Br), 2.2−1.2 (3H, CH_2CH), 1 (3H, CH_3).

Synthesis of Hydroxyl-End-Functionalized Polystyrene. The synthesis was performed according to the procedure shown before with a slight modification.[38,39] The nucleophilic substitution was carried out with a ratio of PS−Br/hydramine = 1/50 in a dilute solution. Taking ethanolamine as an example, the process is briefly described as follows. PS−Br (5.28×10^{-2} mmol, 400 mg, polymer **a**) was dissolved in DMF (8 mL), and then, ethanolamine (2.64 mmol, 158 μL) was added to a 50 mL round-bottom flask. After stirring for 72 h at 40 °C, the reaction mixture was precipitated in methanol. The precipitation procedure was performed three times. The product, ethanolamine-end-functionalized polystyrene (PS−$NHCH_2CH_2OH$, polymer **b**), was dried under a vacuum overnight. The other polystyrenes with different end groups, diethanol amine (PS−$N(CH_2CH_2OH)_2$, polymer **c**), 2-amino-1,3-propanediol (PS−$NHCH(CH_2OH)_2$, polymer **d**), and 2-(2-aminoethoxy) ethanol (PS−$NH(CH_2CH_2O)_2H$, polymer **e**), were obtained with the same process. ^{1}H NMR (500 MHz, $CDCl_3$) δ (ppm): 7.26−6.2 (5H, C_6H_5), 2.2−1.2 (3H, CH_2CH), 1 (3H, CH_3), 3.4−3.25 (2H, CH_2OH for ethanolamine), 3.4−3.25 (4H, 2 × CH_2OH for diethanolamine), 3.4−3.2 (4H, 2 × CH_2OH for 2-amino-1,3-propanediol), 3.7−3.5 (2H, CH_2OH for 2-(2-aminoethoxy)ethanol). The synthesis is depicted in Scheme 1.

Scheme 1. Hydroxyl-Functionalized PS

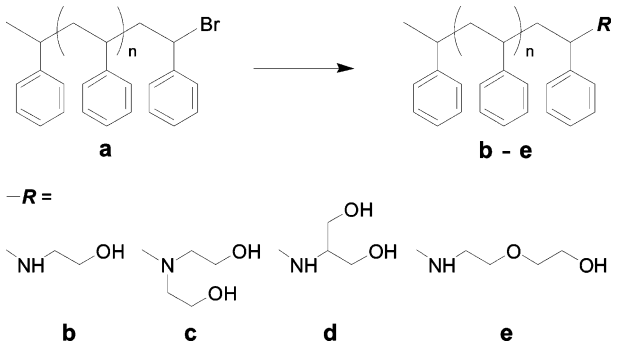

Formation of Honeycomb Films via the Breath Figure Method. The polymers were dissolved in carbon disulfide with different concentrations. An aliquot of 50 μL for each polymer solution was drop-cast onto a PET substrate placed under a 2 L/min humid airflow (25 °C and ∼80% RH). Owing to the condensation of water vapor on the solution surface during the evaporation of carbon disulfide, the transparent solution turned turbid rapidly. After solidification, the film was dried at room temperature.[40]

In Situ Observation of the Breath Figure Process. *In situ* observation of the film formation process was performed under an optical microscope equipped with a digital camera at a magnification of 160. Polymer solutions were cast on PET films fixed on the microscope table under a humid air flow. Videos were started to be recorded about 2 s before the solution was dropped and spread on the substrate and kept recording through the solution hardening. Variation of factors such as air flow rate and the amount of cast polymer solution and its spreading may result in different hardening times. In this work,

dx.doi.org/10.1021/jp4114392 | J. Phys. Chem. B 2014, 118, 845−854

videos were collected under almost the same conditions and should be comparable. We repeated at least five times for each sample, and the typical videos are presented.

Preparation of Dense Films by Spin-Coating. Polymers were dissolved in toluene at a concentration of 10 mg/mL. Flat films were prepared by spin-coating the polymer solutions on silicon wafers at a speed of 2000 rpm, which results in about 36 nm thick films.

Instruments and Measurements. Proton nuclear magnetic resonance (^{1}H NMR) spectra were recorded on a Bruker (Advance DMX500) NMR instrument with tetramethylsilane (TMS) as the internal standard and $CDCl_3$ as the solvent at room temperature.

Molecular weight and molecular weight distribution were measured by a PL 220 gel permeation chromatography (GPC) instrument at 25 °C, which was equipped with a Waters 510 HPLC pump, three Waters Ultrastyragel columns (500, 103, and 105 Å), and a Waters 410 DRI detector. THF was used as the eluent at a flow rate of 1.0 mL/min. The calibration of the molecular weights was based on polystyrene standards.

Matrix-assisted laser desorption ionization time-of-flight mass spectrometry (MALDI-TOF MS) was performed using a Perspective Biosystem Voyager DE-STR MALDI-TOF MS (PE Applied Biosystems, Framingham, MA). A matrix solution of dithranol (20 mg/mL), cationizing salt of silver trifluoroacetate (10 mg/mL), and polymer (10 mg/mL) in THF was mixed in a ratio of 10:2:4, and 0.8 μL of mixed solution was deposited on the sample holder.

The glass transition temperature (T_g) of the polymers was measured by a differential scanning calorimeter (DSC) on a TA Q200 DSC instrument under a nitrogen atmosphere. PS−Br (4.65 mg), PS−$NHCH_2CH_2OH$ (5.1 mg), PS−$N(CH_2CH_2OH)_2$ (4.83 mg), PS−$NHCH(CH_2OH)_2$ (5.13 mg), or PS−$NH(CH_2CH_2O)_2H$ (4.65 mg) was sealed in an aluminum sample crucible under nitrogen protection. Then, the DSC scan was recorded at a heating rate of 10 °C/min from 40 to 150 °C, followed by immediately cooling from 150 to 40 °C at 10 °C/min, and then again heated from 40 to 150 °C at 10 °C/min. The second heating cycle was recorded for T_g measurement.

A field emission scanning electron microscope (FESEM, Sirion-100, FEI) was used to observe the surface morphology of films after being sputtered with gold using ion sputter JFC-1100. The pore diameter and pore center distance were analyzed using ImageTool (v2.0, by UTHSCSA). At least 50 measurements were carried out to calculate the mean value and standard deviation.

Water contact angles were measured on the dense and honeycomb films by a Drop-Meter A-200 contact angle system (MAIST Vision Inspection & Measurement Ltd. Co.) at room temperature. The average values calculated from at least five parallel measurements are reported.

RESULTS AND DISCUSSION

Synthesis and Characterization of Chain-End-Functionalized Polystyrene. Well controlled polymers that contain halide at the chain end can be synthesized via ATRP. The halide can then be converted into various functional groups via nucleophilic substitution.[39,41−44] Combining ATRP with nucleophilic substitution and postreaction, the application of ATRP in designing macromolecule structures can be greatly broadened. In addition, the reaction condition of nucleophilic substitution is mild and not very sensitive to water or oxygen. Here a series of PS−OH were synthesized by the reaction between PS−Br and hydramines. As far as we know, it is the first time to systematically compare the synthesis of polystyrene containing these types of end groups.

PS−Br was synthesized by bulk ATRP using a typical procedure.[26] It has been reported that polymer retains high bromide end-functionality (>90%) when the reaction is stopped at early stages of the polymerization (monomer conversion <30%).[45] In this work, the monomer conversion was controlled at about 27%. And the designed molecular weight (~6000 g/mol, Table 1) was considered to better realize

Table 1. Results of End-Functionalized Polystyrene Prepared by ATRP and Nucleophilic Substitution[a]

sample	$M_{n,GPC}$[b]	M_w/M_n[b]	conv.[c] (%)	T_g[d] (°C)
a	6180	1.07		92.9
b	5450	1.09	>90	93.6
c	5650	1.08	≈60	91.7
d	5700	1.07	≈60	86.0
e	5600	1.08	>90	83.3

[a](a) PS−Br, (b) PS−$NHCH_2CH_2OH$, (c) PS−$N(CH_2CH_2OH)_2$, (d) PS−$NHCH(CH_2OH)_2$, and (e) PS−$NH(CH_2CH_2O)_2H$. [b]GPC using differential refractive index detection vs linear polystyrene standards. [c]Calculated from the ratio of peak area from the ^{1}H NMR spectra. [d]Measured by DSC.

the successful nucleophilic substitution of the end group. Chain-end modification of PS−Br was carried out in the presence of DMF to obtain one or two hydroxyl groups, using a 50 equiv excess of hydramine to kinetically eliminate side reaction. GPC curves (Figure S1 in the Supporting Information) show that the molecular weight of PS−OH was slightly lower than that of PS−Br, which is due to the hydrodynamic volume diminishing induced by the polar end group.

The conversion of the end group was determined by ^{1}H NMR (Figure S2, Supporting Information). The signal from 6.2 to 7.3 ppm is assigned to the aromatic protons. The signal at 1.2−2.2 ppm corresponds to the ethylidene protons. A small peak at around 1.0 ppm is due to the methyl protons of the initiator. After the nucleophilic substitution, we can hardly see the peak of characteristic proton next to the bromine end groups (4.4−4.6 ppm), while new peaks appear between 3.2 and 3.8 ppm, indicating a successful substitution. The end group functionality was calculated from the NMR spectra on the basis of the area ratio of the H_b/H_a and $H_{b'}/H_{a'}$ peaks, i.e., f = functionality (%) = $50H_{b'}H_a/H_bH_{a'}$ for PS−$NHCH_2CH_2OH$ (f_b) and PS−$NH(CH_2CH_2O)_2H$ (f_e) and $25H_{b'}H_a/H_bH_{a'}$ for PS−$N(CH_2CH_2OH)_2$ (f_c) and PS−$NHCH(CH_2OH)_2$ (f_d). Results show that $f_b \approx f_e > 90$ and $f_c \approx f_d \approx 60$. The relatively lower functionality for the latter two samples (**c** and **d**) is attributed to larger steric hindrance and weaker nucleophilicity caused by the two electron-withdrawing hydroxyls.[46] Furthermore, MALDI-TOF MS was used to confirm the end group modification. An apparent advantage of this technique is the signals observed represent the molecular weight of the polymer and the change of the structure of the polymer can be precisely characterized by the shifting of the molecular weight.[47−49]

MALDI-TOF MS spectra (Figure 1) of polystyrenes before and after chain-end modification give similar molecular weight distribution to the GPC traces in Figure S1 (Supporting Information). All of the polymers present a uniform series of

dx.doi.org/10.1021/jp4114392 | J. Phys. Chem. B 2014, 118, 845−854

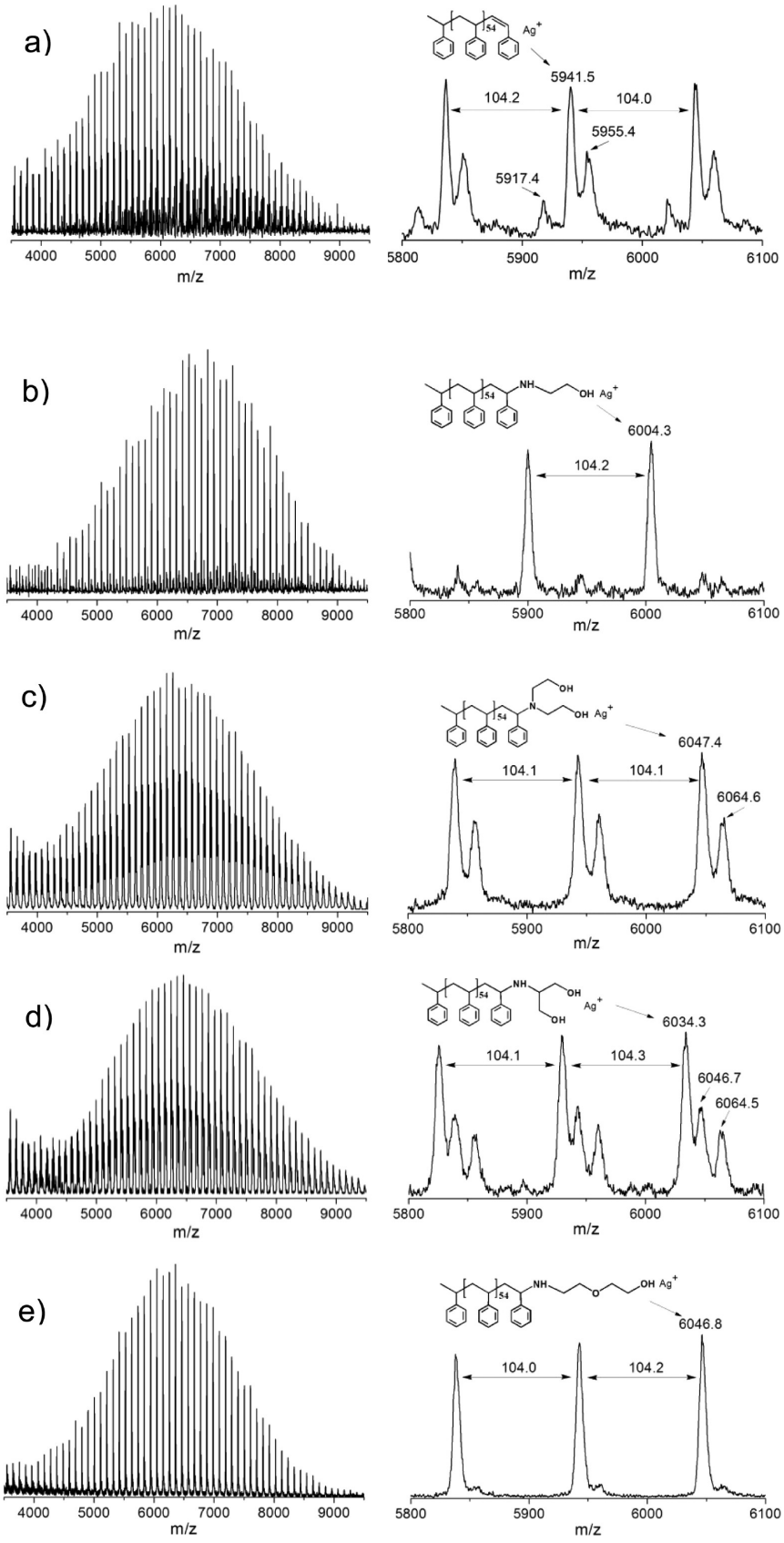

Figure 1. MALDI-TOF MS spectra of PS with different end groups: (a) PS−Br, (b) PS−$NHCH_2CH_2OH$, (c) PS−$N(CH_2CH_2OH)_2$, (d) PS−$NHCH(CH_2OH)_2$, (e) PS−$NH(CH_2CH_2O)_2H$. A range of 5800−6100 m/z is highlighted.

main peaks corresponding to St (peak interval of 104.1 St units). From the magnified region between 5800 and 6100, we can see that the main peaks match the theoretical isotopic pattern very well, confirming the successful modification of

dx.doi.org/10.1021/jp4114392 | J. Phys. Chem. B 2014, 118, 845−854

PS−Br with a series of hydramine. The spectra of polymers **b** and **e** show only a single main peak without other weak peaks, while those of polymers **c** and **d** exhibit some weak peaks with molecular weight shifting. This result is consistent with that of NMR. Moreover, as shown in the spectrum of PS−Br (Figure 1a), a weak peak at −24 m/z [$CH_3CHPh-(CH_2CHPh)_{n-1}-CH_2C(Ph)Br + Ag^+$] with regard to the main peak population [$CH_3CHPh—(CH_2CHPh)_n—CH═C(Ph) + Ag^+$] should be attributed to the part unfragmentation of the C—Br bond, and the peak at +14 m/z can be ascribed to an internal scission of polystyrene chains induced by MALDI-TOF MS [$CH_3CHPh—(CH_2CHPh)_n—CH_2—C(Ph)═CH_2 + Ag^+$].[50,51] The instrumental error is further verified by the nucleophilic substituted polystyrene. For example, a peak shifting of 62.8 m/z can be seen from the spectrum of PS−$NHCH_2CH_2OH$ (Figure 1b) when compared with PS−Br, and apart from the main peaks, no other weak peak can be seen from the spectrum. Specially, only a series of main peaks happen to PS−$NH(CH_2CH_2O)_2H$ (Figure 1e). In addition, the assignment of higher m/z peak at approximately +18 m/z (Figure 1c) with respect to the major peak is unknown but may be related to instrumental conditions, similar observations were also performed by other groups.[51,52] The peak at 6046.7 m/z (Figure 1d) should be attributed to the unreacted polymer of PS−Br. To sum up, the well controlled synthesis of PS−Br and the substitution ratio of PS−OH can be confirmed by the MALDI-TOF MS.

End groups can affect the glass transition temperature (T_g) of polymers.[53−55] DSC curves of the polymers are shown in Figure S3 (Supporting Information). It can be seen from Table 1 that the T_g of PS−Br is 92.9 °C and changes little for PS−$NHCH_2CH_2OH$ (93.6 °C) and PS−$N(CH_2CH_2OH)_2$ (91.7 °C). However, the T_g values of PS−$NHCH(CH_2OH)_2$ and PS−$NH(CH_2CH_2O)_2H$ decrease to 86.0 and 83.3 °C, respectively. The variation in T_g should be attributed to the end groups that can change the free volume of the polymer especially for a polymer with low molecular weight.[55]

Formation of Honeycomb-Patterned Porous Films. It has been reported that ordered honeycomb films can be prepared from amphiphilic polymers because the condensed water droplets can be effectively stabilized by the hydrophilic blocks or groups of the polymers.[56] Figure 2 shows the surface morphology of honeycomb films prepared from the polystyrenes having different end groups. In our case, PS−Br is not able to form ordered porous film at low concentration (2 and 5 mg/mL) because of its poor capacity to stabilize the water droplets. This result is consistent with that reported in the literature.[25,31] As the concentration increases to 8 mg/mL, the film becomes ordered. Meanwhile, highly ordered honeycomb films can be obtained at a low concentration by transferring the bromide end group to one or two hydroxyl groups, which should be attributed to the reduced interfacial tension between the water droplets and the polymer.[56] Moreover, we can get ordered porous films at a wide range of concentrations. It should be noted that almost monodisperse pores were found in the whole film (>15 mm × 15 mm). A typical top-down SEM image showing a large area of perfect honeycomb structure is presented as Figure S4 (Supporting Information). This well ordered honeycomb film is crucial to its applications in fields such as photonic materials, templating, and separation.[16,57,58]

Pore diameter and distance of pore centers were summarized in Figure 3 by analyzing the top-down SEM images. It can be seen that, as expected, the pore diameter decreases by increasing the polymer solution concentration (Figures 2 and 3A). We would like to point out that, if only polymers with

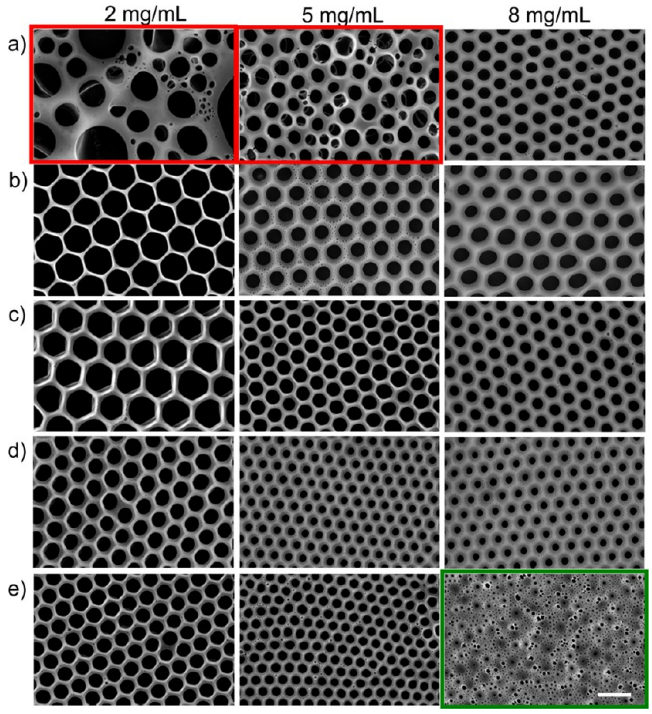

Figure 2. Top-down SEM images of honeycomb porous films prepared from 2, 5, and 8 mg/mL of CS_2 solutions of (a) PS−Br, (b) PS−$NHCH_2CH_2OH$, (c) PS−$N(CH_2CH_2OH)_2$, (d) PS−$NHCH(CH_2OH)_2$, and (e) PS−$NH(CH_2CH_2O)_2H$. The scale bar is 5 μm.

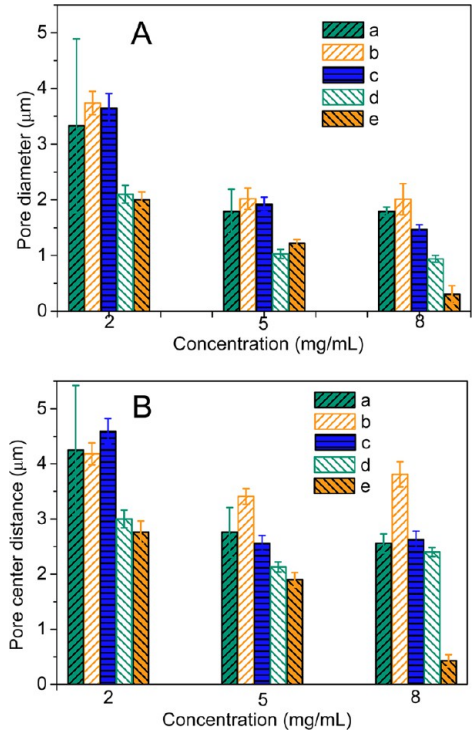

Figure 3. Pore diameter (A) and pore center distance (B) of honeycomb porous films prepared from (a) PS−Br, (b) PS−$NHCH_2CH_2OH$, (c) PS−$N(CH_2CH_2OH)_2$, (d) PS−$NHCH(CH_2OH)_2$, and (e) PS−$NH(CH_2CH_2O)_2H$ at 2, 5, and 8 mg/mL.

dx.doi.org/10.1021/jp4114392 | J. Phys. Chem. B 2014, 118, 845−854

hydrophilic groups are considered, the pore diameter decreases according to the sequence of polymers **b**, **c**, **d**, and **e**. Generally, this phenomenon can be explained on the basis of thermodynamics that polystyrene with more hydrophilic end groups possesses stronger surfactant-like interfacial activity and can thermodynamically stabilize larger interfacial area, leading to smaller pore size. This will be further discussed in the following text.

The cross section views of the films (Figure 4) all exhibit monolayer structure except that prepared from PS−NH-$(CH_2CH_2O)_2H$ at 8 mg/mL, which possesses a multilayer structure. For this sample, the surface pore size ranges from 50 to 500 nm from top view (Figure 2e), and there also exist large pores with a diameter of about 1.5 μm from the cross-sectional view (Figure 4e), which were surrounded by the small pores. The difference between samples shown in Figure 4d and e is that the large pores in Figure 4e are completely sunk into the bulk of the film. We know that the polymers used to prepare the honeycomb films are only slightly different at the polymer chain end. However, changes in the pore diameter, the pore center distance, and the film structure (Figures 2−4) are significant, although they were prepared at the same condition. It is generally accepted that the structures of honeycomb films can be affected by various factors, which include the speed of polymer precipitation at the interface between polymer solution and water droplets and the time scale of water droplet growth and arrangement. To understand the effects of polymer end groups on the film structure, we investigated the polymer properties as well as the film formation process.

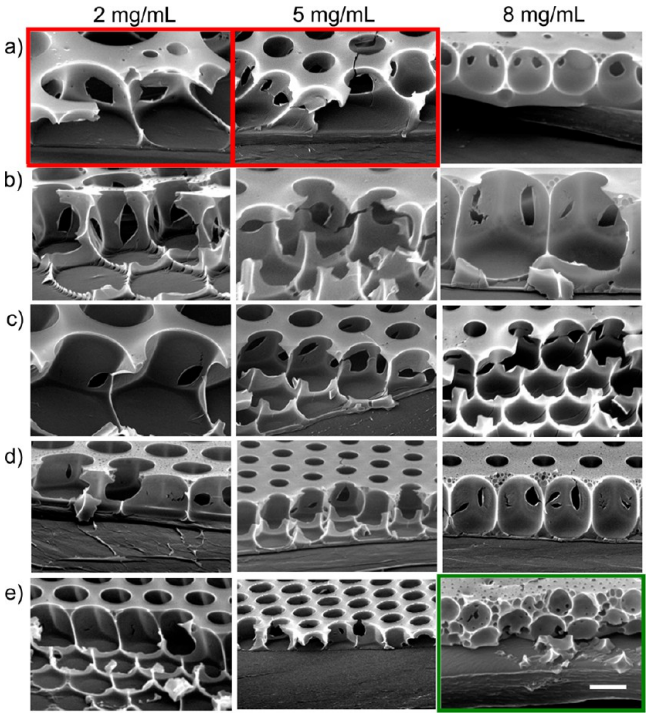

Figure 4. Cross-sectional SEM images of honeycomb porous films prepared from 2, 5, and 8 mg/mL of CS_2 solutions of (a) PS−Br, (b) PS−$NHCH_2CH_2OH$, (c) PS−$N(CH_2CH_2OH)_2$, (d) PS−$NHCH(CH_2OH)_2$, and (e) PS−$NH(CH_2CH_2O)_2H$. The scale bar is 2 μm.

As mentioned above, T_g values of the polymers change with the end groups. Polymers **d** and **e** have relatively lower T_g, which suggests that the mobility of chain segments in these two polymers may be relatively higher. It should be noted that T_g measured in the bulk cannot be directly used to characterize the mobility of polymer in concentrated solution, i.e., in the cast solution suffering solvent evaporation. We further investigated the hydrophilicity of the polymers and the films. The polymers having different end groups also show different hydrophilicity. Dense films were prepared by spin coating of 10 mg/mL polymer solution in toluene at 2000 rpm, on which water contact angles were measured (Table 2). The water contact angle of the most hydrophobic PS−Br dense film (91.2°) is the highest one. After introducing the end groups, the hydrophilicity of all the polymers increases. The water contact angle of PS−$NH(CH_2CH_2O)_2H$ film (polymer **e**) decreases to 85.8°, which is the most hydrophilic. The contact angles of the corresponding honeycomb porous films are in the range 100−130° (Table 2), which is owning to the film surface structure.[22] The water contact angles can be theoretically calculated using Cassie and Baxter's law:

$$\cos\theta_{cal} = (1 - f_{pore}) \times \cos\theta_{polymer} + f_{pore} \times \cos\theta_{pore}$$

where f_{pore} is the area fraction of pores at the surface, $\theta_{polymer}$ is the water contact angle of a polymer in the form of a thin and smooth film, and θ_{pore} is the contact angle of the pore, which is 180° in the Cassie state. f_{pore} was estimated from the SEM images (Figure 5). It can be seen that the calculated results are well consistent with those from experiments except for film prepared from polymer **e** at 8 mg/mL, which is because the irregular surface structure causes deviation for calculating surface pore fraction. It can be concluded that the water contact angles of honeycomb films are mainly affected by the surface topology while those of dense films are determined by the chemistry.

The *in situ* observation of the breath figure process was conducted using polymer solutions with a concentration of 5 mg/mL under an optical microscope equipped with a digital

Table 2. Experimental and Calculated Static Water Contact Angles (CA_{exp} and CA_{cal}) on Honeycomb Films Prepared from PS Having Different End Groups with Concentrations of 2, 5, and 8 mg/mL[a]

	2 mg/mL		5 mg/mL		8 mg/mL		dense film
sample	CA_{exp} (deg)	CA_{cal} (deg)	CA_{exp} (deg)	CA_{cal} (deg)	CA_{exp} (deg)	CA_{cal} (deg)	CA_{exp} (deg)
a	116.2 ± 2.4	117.5	112.3 ± 0.9	114.7	108.9 ± 2.8	112.4	91.2 ± 0.7
b	126.1 ± 2.4	129.3	103.1 ± 1.5	108.9	100.1 ± 2.1	105.4	87.7 ± 0.8
c	127.7 ± 0.7	131.0	119.1 ± 1.3	121.3	109.5 ± 0.3	106.6	88.5 ± 0.2
d	124.9 ± 2.6	117.1	104.8 ± 1.7	102.1	104.3 ± 0.9	98.1	88.7 ± 0.3
e	125.4 ± 2.4	121.2	116.5 ± 2.2	110.1	101.1 ± 0.9	91.7	85.8 ± 0.9

[a]The CA_{exp} on the corresponding dense films were also included. (a) PS−Br, (b) PS−$NHCH_2CH_2OH$, (c) PS−$N(CH_2CH_2OH)_2$, (d) PS−$NHCH(CH_2OH)_2$, and (e) PS−$NH(CH_2CH_2O)_2H$.

dx.doi.org/10.1021/jp4114392 | J. Phys. Chem. B 2014, 118, 845−854

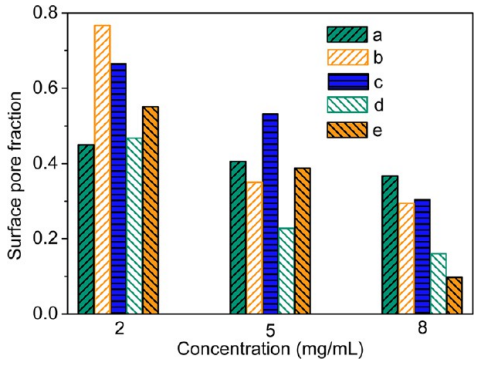

Figure 5. Surface pore fraction of honeycomb films prepared from (a) PS−Br, (b) PS−$NHCH_2CH_2OH$, (c) PS−$N(CH_2CH_2OH)_2$, (d) PS−$NHCH(CH_2OH)_2$, and (e) PS−$NH(CH_2CH_2O)_2H$.

camera. The typical images are shown in Figure 6. At the early stage of the process, a large number of water droplets condense

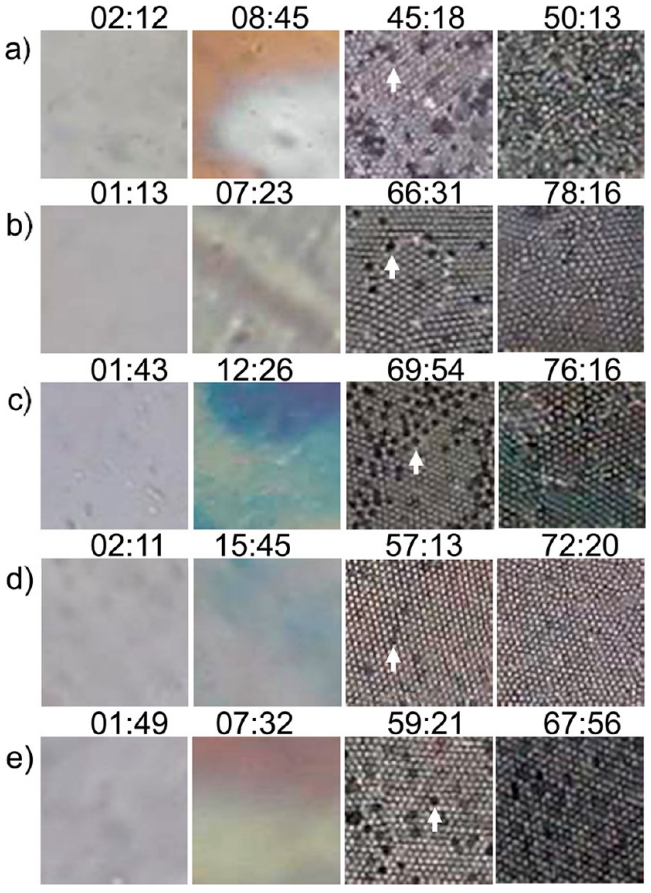

Figure 6. In situ optical micrographs of the breath figure process at different times (seconds). The process was observed by using polymer solutions with a concentration of 5 mg/mL. (a) PS−Br, (b) PS−$NHCH_2CH_2OH$, (c) PS−$N(CH_2CH_2OH)_2$, (d) PS−$NHCH(CH_2OH)_2$, (e) PS−$NH(CH_2CH_2O)_2H$.

onto/into the solution, and the solution changes from homogeneous to opaque. Then, water droplets on the surface grow continuously. The long-range ordering of water droplets is then driven by the thermocapillary effect and Marangoni convection, resulting in a hexagonally close-packed array on the surface of the solution. Finally, solvent evaporates thoroughly, and thin cured film was obtained. In this process, there exists a variety of visible black dots at the surface of the solution as marked by the arrows, which may be pores that are still full of water. The water can migrate from one pore to the other as the pores are interconnected (Figure 4). What interests us more is the fact that the solidification time of the polymers is quite different. The solidification time of PS−Br (~50 s) is greatly shorter than that of the hydroxyl-functionalized polystyrene, all of which exceed 65 s. Longer solidification time suggests longer growing and arranging time of water droplets, which is conducive to the improvement of the regularity of the honeycomb films.

It should be noted that there still exists a partial unreacted end group for polymers **c** and **d**. How does the unreacted end group influence the film structure? To further answer this question, polymers **b** and **e**, which have high conversion ratios, were mixed with PS−Br at different ratios and concentrations. The weight fraction of PS−OH in the mixture varies between 1.0 and 0 at total polymer concentrations of 5 and 8 mg/mL. Figure 7 shows the pore diameter, distance of pore center, and typical SEM images (see also Figure S5, Supporting Information). As mentioned above, films prepared from polymer **e** at 8 mg/mL have unique surface morphology. Similarly, for the studied blends, only polymer **e** at 8 mg/mL shows gradually but obviously increased pore diameter with the addition of PS−Br. In other cases, the pore diameter changes little even when 40% PS−Br was added. As mentioned above, polymers **c** and **d** have a conversion ratio of about 60% and contain about 40% PS−Br. Therefore, it can be concluded that the morphologies of the prepared films are determined to a large extent by the hydrophilic end group in the blends, which makes the relationship between the end groups of the polymers and film morphologies reasonable.

Some Insights into the Formation of Honeycomb-Patterned Porous Films from PS with Different End Groups. As mentioned above, if the environmental conditions keep constant, the morphology of the honeycomb films will be mainly affected by the properties of film-forming polymer through its interaction with the water droplets. For PS−Br, water droplets are mainly stabilized by the polymer precipitates at the water/solution interface due to the hydrophobic nature of the polymer (Figure 8A). When the concentration is as low as 2 or 5 mg/mL, the water droplets cannot be effectively stabilized due to the low segmental density and poor capacity of segmental motion, and hence, coalescence happens continuously, leading to a disordered porous film. As the concentration increases to 8 mg/mL, the segmental density increases. Accordingly, the increased amount of precipitation polymer leads to stabilized water droplets in a shorter period and thus an ordered honeycomb film.

For PS−OH, honeycomb films with large area ordered structure can be achieved because of the reduced interfacial tension by the hydrophilic end group. This interfacial activity makes the polymer spontaneously move toward the solution/water interface and stabilize the water droplets (Figure 8B). This explanation is based on the well-known interfacial thermodynamics and supported by our water contact angle results and partially supported by the T_g analysis. Moreover, the prolonged solidification time also contributes to the ordered structure by extending the time of water droplet growth and arrangement (Figure 6).

It is worth pointing out that all of the prepared films exhibit monolayer structure other than the film prepared from PS−$NH(CH_2CH_2O)_2H$ at 8 mg/mL. That film shows a multilayer

dx.doi.org/10.1021/jp4114392 | J. Phys. Chem. B 2014, 118, 845−854

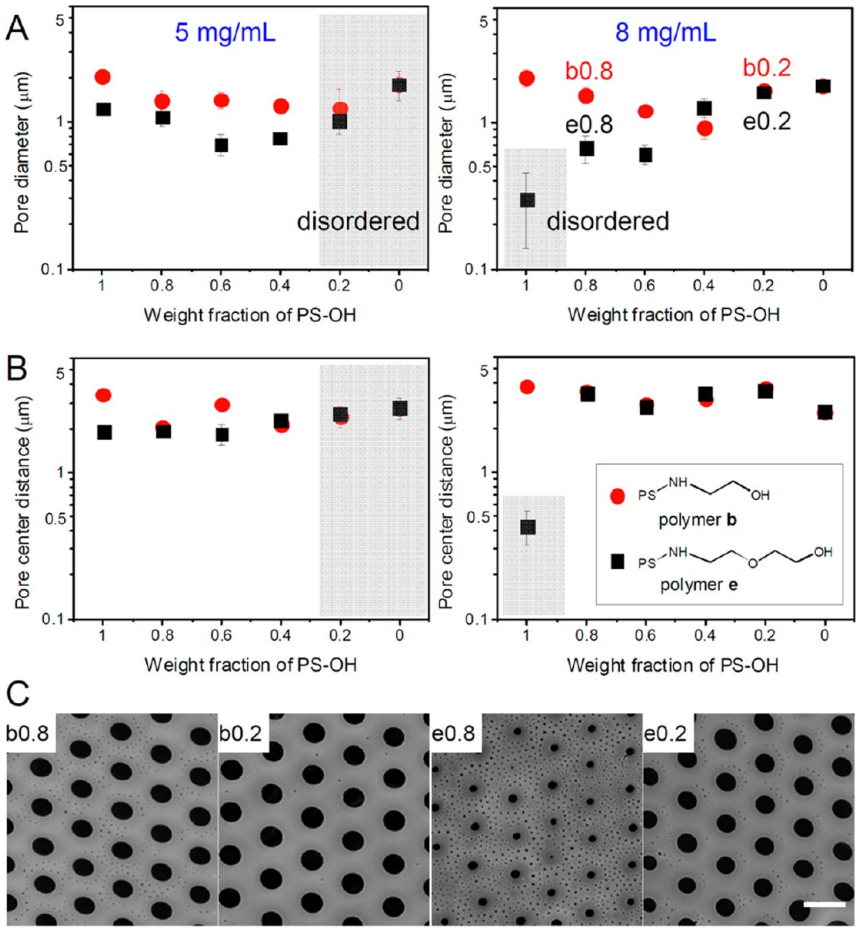

Figure 7. Pore diameter (A) and pore center distance (B) of honeycomb films prepared from the mixture of PS−OH and PS−Br at 5 mg/mL (left panel) and 8 mg/mL (right panel). (C) Typical SEM images of samples prepared from the blends with a total polymer concentration of 8 mg/mL. For example, b0.8 means film prepared from blends in which polymer b has a weight fraction of 0.8. The scale bar is 5 μm.

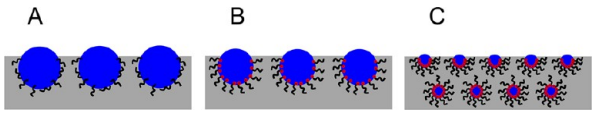

Figure 8. Illustration of self-assembling polymer at the water droplet interfaces during the breath figure process. (A) Polymer without hydrophilic end groups (e.g., PS−Br). (B) Polymer with hydrophilic groups (e.g., PS−$NHCH_2CH_2OH$, PS−$N(CH_2CH_2OH)_2$, and PS−$NHCH(CH_2OH)_2$). (C) Polymer with strong hydrophilic groups (e.g., PS−$NH(CH_2CH_2O)_2H$).

structure and a mean surface pore diameter of about 250 nm. The formation of multilayer structure should be attributed to the stronger ability to stabilize the water droplets by the polymer (Figure 8C) and faster sinking. It has been mentioned above that the segmental mobility of PS−$NH(CH_2CH_2O)_2H$ and its interaction with water droplets are all stronger than the other functionalized polystyrenes. Therefore, the condensed water droplets can be effectively stabilized in a short period and further prohibited from growing at a fast rate. Then, the packaged water droplets are dragged into the solution by the Marangoni effect. Meanwhile, it is difficult for the packaged water droplets to coalesce due to the strong ability of PS−$NH(CH_2CH_2O)_2H$ to stabilize the water droplets. Herein, the submerged water droplets form the first layer. Then, the following condensed water droplets continued to assemble into the solution and solidify on the first layer to form the second layer. This process will continuously happen until the film solidification completes thoroughly, generating the multilayer structured honeycomb film. Bolognesi and the co-workers proposed an equation[59]

$$z_0 = (\gamma_W - \gamma_{W/S})/\gamma_S$$

where γ_W is the water surface tension, γ_S is the solution surface tension, and $\gamma_{W/S}$ is the water/solution interfacial tension. A z_0 value between −1 and 1 indicates that the water droplet is floating at the interface between air and solution; for z_0 greater than 1, water droplets swell below the surface and multilayer structured films can be obtained. Our results support this hypothesis as the most hydrophilic polymer **e** with the largest z_0 value formed multilayer structure. Moreover, because of the shorter growth time of the uppermost water droplets, the nanometer sized surface pore is formed. It is well-known that the breath figure process is controlled by both thermodynamics and kinetics, but it can also be speculated that the kinetics shows greater influences on the outmost pore layer if it is possible to form a multilayer structure.

The results of blend films also support the above-mentioned explanation. By adding 40% hydrophilic PS−OH into PS−Br, the regularity of pore arrays can be greatly improved (Figure 7A, 5 mg/mL). It is because the added PS−OH can help stabilizing condensed water droplets. For the most hydrophilic polymer **e**, only 20% is enough to get nearly ordered film,

dx.doi.org/10.1021/jp4114392 | J. Phys. Chem. B 2014, 118, 845−854

which reveals that polymer **e** is more effective in reducing interface energy.

CONCLUSIONS

A series of end-functionalized polystyrenes synthesized via ATRP of styrene and nucleophilic substitution by four hydramines were used to prepare honeycomb films with large area highly ordered structure at a wide range of concentrations. The hydrophilic end groups can dramatically improve the film-forming property of PS. The regularity of the film is mainly influenced by the interaction of film-forming polymers with condensed water droplets. Polymers with highly similar hydrophilic end groups resulted in greatly different films. Specifically, if the polymer can package the water droplets in a short period, honeycomb film with multilayer structure and nanometer sized surface pores can be formed. Otherwise, only monolayer structure can be formed. For 8 mg/mL polymer **e** that is the most hydrophilic, the addition of PS−Br can gradually increase the pore diameter. This work provides further insight into the intrinsic mechanism of the relationship between the functional end groups and the structure of the honeycomb film, which may allow convenient control over honeycomb films with high reproducibility, high ordering, and complex structures.

ASSOCIATED CONTENT

Supporting Information

GPC traces, ^{1}H NMR spectra, DSC curves, a typical low-magnification SEM image from 8 mg/mL PS−$NHCH_2CH_2OH$ solution, and SEM images of all blend samples. This material is available free of charge via the Internet at http://pubs.acs.org.

AUTHOR INFORMATION

Corresponding Author

*Phone: +86-571-87953763. E-mail: lswan@zju.edu.cn.

Notes

The authors declare no competing financial interest.

ACKNOWLEDGMENTS

This work is supported by the National Natural Science Foundation of China (21374100 and 51173161). We thank Dr. Guowei Wang at the Department of Macromolecular Science, Fudan University, for MALDI-TOF analysis.

REFERENCES

(1) Widawski, G.; Rawiso, M.; Francois, B. Self-Organized Honeycomb Morphology of Star-Polymer Polystyrene Films. *Nature* **1994**, *369*, 387−389.

(2) Wan, L. S.; Li, Q. L.; Chen, P. C.; Xu, Z. K. Patterned Biocatalytic Films via One-Step Self-Assembly. *Chem. Commun.* **2012**, *48*, 4417−4419.

(3) Gong, J.; Sun, L.; Zhong, Y.; Ma, C.; Li, L.; Xie, S.; Svrcek, V. Fabrication of Multi-Level Carbon Nanotube Arrays with Adjustable Patterns. *Nanoscale* **2012**, *4*, 278−283.

(4) Lu, M. H.; Zhang, Y. Microbead Patterning on Porous Films with Ordered Arrays of Pores. *Adv. Mater.* **2006**, *18*, 3094.

(5) Li, X.; Zhang, L.; Wang, Y.; Yang, X.; Zhao, N.; Zhang, X.; Xu, J. A Bottom-up Approach to Fabricate Patterned Surfaces with Asymmetrical TiO_2 Microparticles Trapped in the Holes of Honeycomb-Like Polymer Film. *J. Am. Chem. Soc.* **2011**, *133*, 3736−3739.

(6) Song, L.; Bly, R. K.; Wilson, J. N.; Bakbak, S.; Park, J. O.; Srinivasarao, M.; Bunz, U. H. F. Facile Microstructuring of Organic Semiconducting Polymers by the Breath Figure Method: Hexagonally Ordered Bubble Arrays in Rigid-Rod Polymers. *Adv. Mater.* **2004**, *16*, 115−118.

(7) Hsu, J.-C.; Sugiyama, K.; Chiu, Y.-C.; Hirao, A.; Chen, W.-C. Synthesis of New Star-Shaped Polymers with Styrene-Fluorene Conjugated Moieties and Their Multicolor Luminescent Ordered Microporous Films. *Macromolecules* **2010**, *43*, 7151−7158.

(8) Wang, J.; Shen, H.-X.; Wang, C.-F.; Chen, S. Multifunctional Ionomer-Derived Honeycomb-Patterned Architectures and Their Performance in Light Enhancement of Light-Emitting Diodes. *J. Mater. Chem.* **2012**, *22*, 4089−4096.

(9) Chen, P. C.; Wan, L. S.; Ke, B. B.; Xu, Z. K. Honeycomb-Patterned Film Segregated with Phenylboronic Acid for Glucose Sensing. *Langmuir* **2011**, *27*, 12597−12605.

(10) Zander, N. E.; Orticki, J. A.; Karikari, A. S.; Long, T. E.; Rawlett, A. M. Super-Hydrophobic Surfaces via Micrometer-Scale Templated Pillars. *Chem. Mater.* **2007**, *19*, 6145−6149.

(11) Ishii, D.; Yabu, H.; Shimomura, M. Novel Biomimetic Surface Based on a Self-Organized Metal-Polymer Hybrid Structure. *Chem. Mater.* **2009**, *21*, 1799−1801.

(12) Brown, P. S.; Talbot, E. L.; Wood, T. J.; Bain, C. D.; Badyal, J. P. S. Superhydrophobic Hierarchical Honeycomb Surfaces. *Langmuir* **2012**, *28*, 13712−13719.

(13) Beattie, D.; Wong, K. H.; Williams, C.; Poole-Warren, L. A.; Davis, T. P.; Barner-Kowollik, C.; Stenzel, M. H. Honeycomb-Structured Porous Films from Polypyrrole-Containing Block Copolymers Prepared via RAFT Polymerization as a Scaffold for Cell Growth. *Biomacromolecules* **2006**, *7*, 1072−1082.

(14) Fukuhira, Y.; Ito, M.; Kaneko, H.; Sumi, Y.; Tanaka, M.; Yamamoto, S.; Shimomura, M. Prevention of Postoperative Adhesions by a Novel Honeycomb-Patterned Poly(Lactide) Film in a Rat Experimental Model. *J. Biomed. Mater. Res., Part B* **2008**, *86*, 353−359.

(15) Ke, B. B.; Wan, L. S.; Xu, Z. K. Controllable Construction of Carbohydrate Microarrays by Site-Directed Grafting on Self-Organized Porous Films. *Langmuir* **2010**, *26*, 8946−8952.

(16) Wan, L. S.; Li, J. W.; Ke, B. B.; Xu, Z. K. Ordered Microporous Membranes Templated by Breath Figures for Size-Selective Separation. *J. Am. Chem. Soc.* **2012**, *134*, 95−98.

(17) Cong, H.; Wang, J.; Yu, B.; Tang, J. Preparation of a Highly Permeable Ordered Porous Microfiltration Membrane of Brominated Poly(phenylene oxide) on an Ice Substrate by the Breath Figure Method. *Soft Matter* **2012**, *8*, 8835−8839.

(18) Du, C.; Zhang, A.; Bai, H.; Li, L. Robust Microsieves with Excellent Solvent Resistance: Cross-Linkage of Perforated Polymer Films with Honeycomb Structure. *ACS Macro Lett.* **2013**, *2*, 27−30.

(19) Li, L.; Chen, C.; Li, J.; Zhang, A.; Liu, X.; Xu, B.; Gao, S.; Jin, G.; Ma, Z. Robust and Hydrophilic Polymeric Films with Honeycomb Pattern and Their Cell Scaffold Applications. *J. Mater. Chem.* **2009**, *19*, 2789−2796.

(20) Kim, J.; Serpe, M. J.; Lyon, L. A. Photoswitchable Microlens Arrays. *Angew. Chem., Int. Ed.* **2005**, *44*, 1333−1336.

(21) Lee, S.-K.; Yi, G.-R.; Moon, J. H.; Yang, S.-M.; Pine, D. J. Pixellated Photonic Crystal Films by Selective Photopolymerization. *Adv. Mater.* **2006**, *18*, 2111−2116.

(22) Ting, W.-H.; Chen, C.-C.; Dai, S. A.; Suen, S.-Y.; Yang, I. K.; Liu, Y.-L.; Chen, F. M. C.; Jeng, R.-J. Superhydrophobic Waxy-Dendron-Grafted Polymer Films via Nanostructure Manipulation. *J. Mater. Chem.* **2009**, *19*, 4819−4828.

(23) Ke, B. B.; Wan, L. S.; Chen, P. C.; Zhang, L. Y.; Xu, Z. K. Tunable Assembly of Nanoparticles on Patterned Porous Film. *Langmuir* **2010**, *26*, 15982−15988.

(24) Ke, B. B.; Wan, L. S.; Li, Y.; Xu, M. Y.; Xu, Z. K. Selective Layer-by-Layer Self-Assembly on Patterned Porous Films Modulated by Cassie-Wenzel Transition. *Phys. Chem. Chem. Phys.* **2011**, *13*, 4881−4887.

(25) Peng, J.; Han, Y. C.; Yang, Y. M.; Li, B. Y. The Influencing Factors on the Macroporous Formation in Polymer Films by Water Droplet Templating. *Polymer* **2004**, *45*, 447−452.

(26) Ke, B. B.; Wan, L. S.; Zhang, W. X.; Xu, Z. K. Controlled Synthesis of Linear and Comb-Like Glycopolymers for Preparation of Honeycomb-Patterned Films. *Polymer* **2010**, *51*, 2168−2176.
(27) Ferrari, E.; Fabbri, P.; Pilati, F. Solvent and Substrate Contributions to the Formation of Breath Figure Patterns in Polystyrene Films. *Langmuir* **2011**, *27*, 1874−1881.
(28) Wang, Z. L.; Xu, J. T.; Du, B. Y.; Fan, Z. Q. Preparation and Characterization of V-Shaped PS-b-PEO Brushes Anchored on Planar Gold Substrate through the Trithiocarbonate Junction Group. *J. Colloid Interface Sci.* **2012**, *384*, 29−37.
(29) Nishikawa, T.; Ookura, R.; Nishida, J.; Arai, K.; Hayashi, J.; Kurono, N.; Sawadaishi, T.; Hara, M.; Shimomura, M. Fabrication of Honeycomb Film of an Amphiphilic Copolymer at the Air-Water Interface. *Langmuir* **2002**, *18*, 5734−5740.
(30) Ma, H.; Hao, J. Evaporation-Induced Ordered Honeycomb Structures of Gold Nanoparticles at the Air/Water Interface. *Chem.—Eur. J.* **2010**, *16*, 655−660.
(31) Billon, L.; Manguian, M.; Pellerin, V.; Joubert, M.; Eterradossi, O.; Garay, H. Tailoring Highly Ordered Honeycomb Films Based on Ionomer Macromolecules by the Bottom-up Approach. *Macromolecules* **2009**, *42*, 345−356.
(32) Galeotti, F.; Calabrese, V.; Cavazzini, M.; Quici, S.; Poleunis, C.; Yunus, S.; Bolognesi, A. Self-Functionalizing Polymer Film Surfaces Assisted by Specific Polystyrene End-Tagging. *Chem. Mater.* **2010**, *22*, 2764−2769.
(33) Hernandez-Guerrero, M.; Davis, T. P.; Barner-Kowollik, C.; Stenzel, M. H. Polystyrene Comb Polymers Built on Cellulose or Poly(styrene-*co*-2-hydroxyethylmethacrylate) Backbones as Substrates for the Preparation of Structured Honeycomb Films. *Eur. Polym. J.* **2005**, *41*, 2264−2277.
(34) Vivek, A. V.; Babu, K.; Dhamodharan, R. Arborescent Polystyrene via Ambient Temperature ATRP: Toward Ordered Honeycomb Microstructured Templates. *Macromolecules* **2009**, *42*, 2300−2303.
(35) Stenzel-Rosenbaum, M. H.; Davis, T. P.; Fane, A. G.; Chen, V. Porous Polymer Films and Honeycomb Structures Made by the Self-Organization of Well-Defined Macromolecular Structures Created by Living Radical Polymerization Techniques. *Angew. Chem., Int. Ed.* **2001**, *40*, 3428−3432.
(36) Connal, L. A.; Vestberg, R.; Hawker, C. J.; Qiao, G. G. Dramatic Morphology Control in the Fabrication of Porous Polymer Films. *Adv. Func. Mater.* **2008**, *18*, 3706−3714.
(37) Zhu, L. W.; Wan, L. S.; Jin, J.; Xu, Z. K. Honeycomb Porous Films Prepared from Porphyrin-Cored Star Polymers: Submicrometer Pores Induced by Transition of Monolayer into Multilayer Structures. *J. Phys. Chem. C* **2013**, *117*, 6185−6194.
(38) Matmour, R.; Lepoittevin, B.; Joncheray, T. J.; El-Khouri, R. J.; Taton, D.; Duran, R. S.; Gnanou, Y. Synthesis and Investigation of Surface Properties of Dendrimer-Like Copolymers Based on Polystyrene and Poly(tert-butylacrylate). *Macromolecules* **2005**, *38*, 5459−5467.
(39) Babin, J.; Leroy, C.; Lecommandoux, S.; Borsali, R.; Gnanou, Y.; Taton, D. Towards an Easy Access to Amphiphilic Rod-Coil Miktoarm Star Copolymers. *Chem. Commun.* **2005**, 1993−1995.
(40) Wan, L. S.; Ke, B. B.; Li, X. K.; Meng, X. L.; Zhang, L. Y.; Xu, Z. K. Honeycomb-Patterned Films of Polystyrene/Poly(ethylene glycol): Preparation, Surface Aggregation and Protein Adsorption. *Sci. China: Chem.* **2009**, *52*, 969−974.
(41) Coessens, V.; Matyjaszewski, K. Synthesis of Polymers with Hydroxyl End Groups by Atom Transfer Radical Polymerization. *Macromol. Rapid Commun.* **1999**, *20*, 127−134.
(42) Lutz, J.-F. 1,3-Dipolar Cycloadditions of Azides and Alkynes: A Universal Ligation Tool in Polymer and Materials Science. *Angew. Chem., Int. Ed.* **2007**, *46*, 1018−1025.
(43) Xu, J.; Ye, J.; Liu, S. Synthesis of Well-Defined Cyclic Poly(N-isopropylacrylamide) via Click Chemistry and Its Unique Thermal Phase Transition Behavior. *Macromolecules* **2007**, *40*, 9103−9110.
(44) Rao, J.; Zhang, Y.; Zhang, J.; Liu, S. Facile Preparation of Well-Defined Ab(2) Y-Shaped Miktoarm Star Polypeptide Copolymer via the Combination of Ring-Opening Polymerization and Click Chemistry. *Biomacromolecules* **2008**, *9*, 2586−2593.
(45) Hong, S. C.; Lutz, J. F.; Inoue, Y.; Strissel, C.; Nuyken, O.; Matyjaszewski, K. Use of an Immobilized/Soluble Hybrid ATRP Catalyst System for the Preparation of Block Copolymers, Random Copolymers, and Polymers with High Degree of Chain End Functionality. *Macromolecules* **2003**, *36*, 1075−1082.
(46) Pioge, S.; Fontaine, L.; Soutif, J. C.; Nicol, E.; Pascual, S. A New Strategy for the Synthesis of Methacrylate End-Functionalized Macromonomers by ATRP. *J. Polym. Sci., Part A: Polym. Chem.* **2010**, *48*, 1526−1537.
(47) Francis, R.; Lepoittevin, B.; Taton, D.; Gnanou, Y. Toward an Easy Access to Asymmetric Stars and Miktoarm Stars by Atom Transfer Radical Polymerization. *Macromolecules* **2002**, *35*, 9001−9008.
(48) Fan, X. S.; Huang, B.; Wang, G. W.; Huang, J. L. Synthesis of Amphiphilic Heteroeight-Shaped Polymer Cyclic- Poly(ethylene oxide)-*b*-Polystyrene (2) via "Click" Chemistry. *Macromolecules* **2012**, *45*, 3779−3786.
(49) Fan, X. S.; Huang, B.; Wang, G. W.; Huang, J. L. Synthesis of Biocompatible Tadpole-Shaped Copolymer with One Poly(ethylene oxide) (PEO) Ring and Two Poly(epsilon-caprolactone) (PCL) Tails by Combination of Glaser Coupling with Ring-Opening Polymerization. *Polymer* **2012**, *53*, 2890−2896.
(50) Pascual, S.; Coutin, B.; Tardi, M.; Polton, A.; Vairon, J. P.; Chiarelli, R. Kinetic and Mechanistic Study of Copper Chloride-Mediated Atom Transfer Polymerization of Styrene in the Presence of N,N-Dimethylformamide. *Macromolecules* **2001**, *34*, 5752−5758.
(51) Ladaviere, C.; Lacroix-Desmazes, P.; Delolme, F. First Systematic MALDI/ESI Mass Spectrometry Comparison to Characterize Polystyrene Synthesized by Different Controlled Radical Polymerizations. *Macromolecules* **2009**, *42*, 70−84.
(52) Kulis, J.; Bell, C. A.; Micallef, A. S.; Jia, Z. F.; Monteiro, M. J. Rapid, Selective, and Reversible Nitroxide Radical Coupling (NRC) Reactions at Amibient Temperature. *Macromolecules* **2009**, *42*, 8218−8227.
(53) Orlicki, J. A.; Thompson, J. L.; Markoski, L. J.; Sill, K. N.; Moore, J. S. Synthesis and Characterization of End-Group Modified Hyperbranched Polyetherimides. *J. Polym. Sci., Part A: Polym. Chem.* **2002**, *40*, 936−946.
(54) Tande, B. M.; Wagner, N. J.; Kim, Y. H. Influence of End Groups on Dendrimer Rheology and Conformation. *Macromolecules* **2003**, *36*, 4619−4623.
(55) Sinnwell, S.; Ritter, H. Microwave Accelerated Polymerization of 2-Phenyl-5,6-dihydro-4h-1,3-oxazine: Kinetics and Influence of End-Groups on Glass Transition Temperature. *Macromol. Rapid Commun.* **2006**, *27*, 1335−1340.
(56) Maruyama, N.; Koito, T.; Nishida, J.; Sawadaishi, T.; Cieren, X.; Ijiro, K.; Karthaus, O.; Shimomura, M. Mesoscopic Patterns of Molecular Aggregates on Solid Substrates. *Thin Solid Films* **1998**, *327*, 854−856.
(57) Heng, L. P.; Zhai, J.; Zhao, Y.; Xu, J. J.; Sheng, X. L.; Jiang, L. Enhancement of Photocurrent Generation by Honeycomb Structures in Organic Thin Films. *ChemPhysChem* **2006**, *7*, 2520−2525.
(58) Yunus, S.; Spano, F.; Patrinoiu, G.; Bolognesi, A.; Botta, C.; Bruhwiler, D.; Ruiz, A. Z.; Calzaferri, G. Hexagonal Network Organization of Dye-Loaded Zeolite L Crystals by Surface-Tension-Driven Autoassembly. *Adv. Funct. Mater.* **2006**, *16*, 2213−2217.
(59) Bolognesi, A.; Mercogliano, C.; Yunus, S.; Civardi, M.; Comoretto, D.; Turturro, A. Self-Organization of Polystyrenes into Ordered Microstructured Films and Their Replication by Soft Lithography. *Langmuir* **2005**, *21*, 3480−3485.